



The effect of using water/CuO nanofluid and L-shaped porous ribs on the performance evaluation criterion of microchannels

Davood Toghraie¹ · Mohammad Mahmoudi² · Omid Ali Akbari² · Farzad Pourfattah³ · Mousa Heydari²

Received: 28 November 2017 / Accepted: 4 April 2018 / Published online: 17 April 2018
© Akadémiai Kiadó, Budapest, Hungary 2018

Abstract

The main purpose of this study is numerically investigating the flow and heat transfer of nanofluid flow inside a microchannel with L-shaped porous ribs as well as studying the effect of porous media properties on the performance evaluation criterion (PEC) of the fluid. In the present paper, in addition to the pure water fluid, the effect of using water/CuO nanofluid on the PEC of microchannel was investigated. The flow was simulated in four Reynolds numbers and two different volume fractions of nanoparticles in laminar flow regime. The investigated parameters are the thermal conductivity and the porosity rate of porous medium. The results indicate that with the existence of porous ribs, the nanofluid does not have a significant effect on heat transfer increase. By using porous ribs in flow with Reynolds number of 1200, the heat transfer rate increases up to 42% and in flow with Reynolds number of 100, this rate increases by 25%.

Keywords Nanofluid · Microchannel · Porous ribs · Performance evaluation criterion (PEC)

List of symbols

C_p	Heat capacity ($\text{J kg}^{-1} \text{K}^{-1}$)
D_h	Hydraulic diameter (m)
f	Friction factor
H	Convective heat transfer coefficient ($\text{W m}^{-2} \text{K}^{-1}$)
K	Thermal conductivity ($\text{W m}^{-1} \text{K}^{-1}$)
Nu	Nusselt number
q''	Thermal heat flux (W m^{-2})
Re	Reynolds number
PEC	Performance evaluation criterion
T	Temperature (K)
P_p	Pumping power (W)
P	Pressure (Pa)
U	Velocity component along the x (m s^{-1})
V	Velocity component along the y (m s^{-1})
w	Velocity component along the z (m s^{-1})

Greek symbols

ρ	Density (kg m^{-3})
μ	Dynamic viscosity (Pa s)
ε	Porosity coefficient
φ	Nanoparticles volume fraction

Super- and subscripts

Ave	Average
B	Balk
f	Base fluid (pure water)
nf	Nanofluid
P	Solid nanoparticles

Introduction

Among the conventional techniques of heat transfer increase, adding metal or non-metal nanoparticles to the special type of fluids, called nanofluid, has particular importance. The use of microchannel as a novel heat transfer equipment has become widespread in modern miniature industries, and the convection heat transfer in porous media saturated by fluid is the main subject of recent studies. It has been shown that porous media have a high efficiency of heat transfer increase. Researchers have focused on the convection heat transfer in porous media because of its wide usage in thermal engineering fields,

✉ Davood Toghraie
Toghraee@iaukhsh.ac.ir

¹ Department of Mechanical Engineering, Khomeinishahr Branch, Islamic Azad University, Khomeinishahr 84175-119, Iran

² Young Researchers and Elite Club, Khomeinishahr Branch, Islamic Azad University, Khomeinishahr, Iran

³ Department of Mechanical and Aerospace Engineering, Malek-Ashtar University of Technology, Shahin-shahr, Isfahan, Iran

such as the geothermal systems, oil extracting, heat exchangers, thermal insulation, maintenance of nuclear wastes, dehumidifying or drying processes, air heaters and porous journal bearings [1].

In this study, the effect of porous medium and nanofluid on the characteristics of flow and heat transfer was investigated and we will review some studies investigating two areas: (1) studies describing the porous media and (2) studies investigating the nanofluid behavior.

In the engineering applications, the heat transfer of porous media has great importance; therefore, many researchers have studied the heat transfer in porous media with different geometries. Poulikakos and Kazmierczak [2] studied the convection heat transfer in two channels, one with parallel plates and the other one with a circular section. Alkam et al. [3] investigated the forced convection heat transfer in the developed region of a channel partially filled with porous materials. The important results of the mentioned reference are that the maximum rate of Nusselt number is related to the channel filled with porous material and in the inertia coefficients higher than 1000, the effect of Darcy number becomes insignificant. Therefore, by using porous material with high thermal conductivity, by reducing Darcy number and increasing the microscopic inertia coefficient, heat transfer increases.

Other works focusing on usage of porous materials are mentioned here. Alkam and Al-Nimr [4] introduced a novel method for substituting porous material on each side of internal walls of a concentric tubular exchanger. Their numerical method showed that although the pressure drop increases correspondingly, the use of porous blocks has a great effect on exchanger efficiency. Jiang and Ren [5] studied the flow and heat transfer in a channel completely filled with porous material under the constant heat flux. Their results showed that by using a numerical method and transient thermal model and also applying constant heat flux boundary condition to the walls, the convection heat transfer of porous medium can be predicted. Lee et al. [6] studied the convection heat transfer in a channel filled with porous material and calculated the thickness of momentum boundary layer as the function of Reynolds and Darcy numbers. Mohamad et al. [7] investigated the heat transfer increase in a tube and channel completely or partially filled with porous material in the laminar flow regime. They observed that, unlike the pressure drop increase, by placing porous material at the center of channel the heat transfer increases logically and the length of developed thermal region increases by 50% or more. Kuznetsov et al. [8] numerically investigated the heat transfer of turbulent flow in a channel with porous material and for modeling the turbulent flow, they used the k - ϵ model. They concluded that, comparing to the interface condition, Nusselt number has a minimal rate of increase. Vafai and Haji-Sheikh [9]

studied the heat transfer of flow crossing from a channel filled with porous material having different lateral sections. They also investigated channels with parallel plates and circular tubes and obtained an accurate numerical solution for these two cases. Forooghi et al. [10] investigated the heat transfer of steady and unsteady pulsating flows in a channel partially filled with porous material with unbalanced thermal conditions. They concluded that, by increasing the conductivity ratio, heat transfer is increased. Hetsrony et al. [11] experimentally studied the heat transfer and pressure drop in a rectangular channel with porous material for removing heat from high powered tools. Their results showed that, although with the additional of heat transfer the pumping power becomes higher, the heat sink still has a high efficiency. Yang and Hwang [12] studied the behavior of turbulent flow and heat transfer increase at the center of a tube completely and partially filled with porous material. They concluded that by increasing Reynolds number and the thickness of porous medium, Nusselt number is increased. However, by increasing Darcy number Nusselt number reduces.

Other papers focusing on both porosity and nanofluids applications also need to be mentioned. Nazari et al. [13] studied the heat transfer of water/CuO nanofluid in two-dimensional sinusoidal and porous channels. Their numerical results showed that by using porosity and nanofluid in these channels, Nusselt number and convection heat transfer coefficient are increased. Li and Kleinstreuer [14] studied the heat transfer performance in a microchannel and concluded that comparing to the pure water fluid, using water/CuO nanofluid improves the heat transfer performance. Chein and Chung [15] investigated the heat transfer performance in a microchannel heat sink. They concluded that compared with the pure water fluid, the best heat transfer performance of water/CuO nanofluid arises in low flow rates. Barzegarian et al. [16] experimentally investigated the effect of employing water/TiO₂ nanofluid on thermal-hydraulic characteristics of a brazed plate heat exchanger used in domestic hot water system in the turbulent flow regime. They observed that the convection heat transfer coefficient of nanofluid increases as Reynolds number rises and in a specific Reynolds number, by increasing volume fraction of nanoparticles, the heat transfer characteristics are increased. He also reported that the convection heat transfer coefficient of nanofluid in 1.5 mass% is almost 23.7% higher than the base fluid.

In order to compare the effect of nanofluid compared with pure water as coolant, the following papers can be cited: Jung et al. [17] and Ho et al. [18] studied the cooling nanofluid performance of forced flow inside the microchannel they reported that comparing to the pure water, water/Al₂O₃ nanofluid has higher heat transfer efficiency in microchannel. Bhattacharya et al. [19] studied

the heat transfer of turbulent nanofluid flow in a microchannel and concluded that using water/ Al_2O_3 nanofluid causes the increase in thermal performance in microchannel heat sink. Sheikhzaseh et al. [20] studied the pressure drop and heat transfer of nanofluid inside the microchannel. They reported that although increasing volume fraction of nanoparticles causes the increase in heat transfer, the pressure drop increases as well. Also, using nanofluid in higher Reynolds numbers compared to lower ones causes greater increase in Nusselt number. Abdollahi et al. [21] numerically investigated the heat transfer of nanofluid in a microchannel heat sink and concluded that the increase in volume fraction and solid nanoparticles diameter do not have a significant effect on the pressure drop coefficient. Lelea et al. [22] studied the performance of nanofluid flow in a microchannel heat sink and reported that the increasing nanoparticles concentration improves heat transfer. Also, the heat transfer coefficients in heating and cooling states are 9 and 20% more than the pure water, respectively. Sakanova et al. [23] studied the improvement in heat transfer performance of nanofluid in a wavy channel and compared the obtained results with a rectangular channel. They reported that in channel with sinusoidal walls, compared to the channel with flat walls, the heat transfer improves significantly; but the use of nanofluid in the sinusoidal channel does not have any considerable effect on heat transfer increase. Benjamin Rimbault et al. [24] experimentally investigated the effect of nanofluid on heat transfer and concluded that compared with pure water fluid, the heat transfer, the friction coefficient and pressure drop increase significantly in low volume fractions.

Further works that focused on several heat transfer efficiency indices for microchannels deserve to be mentioned here as well. Li et al. [25] analyzed the heat transfer of nanofluid flow in a microchannel with dimples and protrusions. They reported that by increasing the volume fraction, heat transfer increases and wall temperature decreases. Also, Diao et al. [26] studied the heat transfer performance in a device with a rectangular microchannel. They reported that water/ Al_2O_3 nanofluid has better heat transfer compared with pure water fluid in a microchannel. Mital [27] analytically studied the heat transfer of water/ Al_2O_3 nanofluid flow and the pumping power in a microchannel and concluded that, although the increase in volume fraction of nanoparticle in the base fluid results in higher heat transfer, it does not have any considerable effect on pumping power. Ming et al. [28] simulated the laminar flow in a tube with metal porous medium and high thermal conductivity and showed that uniform temperature distribution is obtained after filling the tube with porous material and the Nusselt number increases significantly. Peng et al. [29] investigated the influence of thermal

conductivity of porous medium on flow and heat transfer characteristics. The most important parameters that they analyzed are Nusselt number and the performance evaluation. Their results showed that Nusselt number and PEC of ETfHE neither increase monotonically with the thermal conductivity of porous medium nor increase monotonically with Reynolds number. Akbari et al. [30–34] numerically investigated the nanofluid flow in a microchannel and microtube in two- and three-dimensional geometries. Their results showed that increasing the volume fraction of nanoparticles increases heat transfer and friction coefficient of microchannel walls. Also, the increase in these two parameters is higher in the indented microchannel compared with the flat one.

By reviewing reliable references, it was determined that the use of porous media and cooling surface of nanofluid was widely investigated by researchers. Due to the presence of sharp walls, there is less heat transfer in the checked channel. This behavior results from a reduction in the heat transfer coefficient in these areas. In order to better distribute heat and eliminate these hot areas, in this paper, part of the corners of the surface is filled with porous materials. This idea can be used in the industry and in areas where there is a lack of heat transfer. In the present paper, the effect of using microchannel with porous ribs on heat transfer rate was studied. Additionally, in order to determine the effect of simultaneous use of porous medium and nanofluid, the effect of adding CuO nanoparticles to the base fluid was also simulated by using finite volume method. Results are provided for different parameters such as Nusselt number, friction coefficient and the performance evaluation criterion (PEC). Also, Reynolds numbers, volume fractions, porosity coefficients and various thermal conductivity coefficients were compared. In the present study, the contours of static temperature distribution on channel floor were presented and compared in different thermal conductivities of porous ribs. By considering all of the mentioned parameters in the rectangular channel with porous ribs, the present study distinguishes itself from the papers from other researchers.

Problem statement and studied geometry

In present study, the flow and heat transfer of water/CuO nanofluid inside the microchannel with L-shaped porous ribs was investigated with two different volume fractions of CuO nanoparticles in water as the base fluid under the constant heat flux. The objective of present study is investigating the effect of porous medium properties, such as the porosity coefficient and thermal conductivity as well as the effect of CuO nanoparticles on heat transfer increase rate. For this reason, the L-shaped ribs were placed inside

the microchannel and the flow was analyzed Reynolds numbers of 100, 300, 600 and 1200 and volume fractions of 0, 2 and 4% of CuO nanoparticles in laminar flow regime. The geometry of L-shaped ribs is shown in Fig. 1 and Table 1. The porosity coefficients of the indented porous medium are 0.5 and 0.8 with thermal conductivities of 7.5 and 15 W m⁻¹ K⁻¹.

Governing equations

The governing equations of fluid flow are Navier–Stokes equations. The physical properties of porous material are presented as the functions of porosity rate, fluid and solid material properties. The fluid flow is determined by the continuity, momentum and energy equations [35].

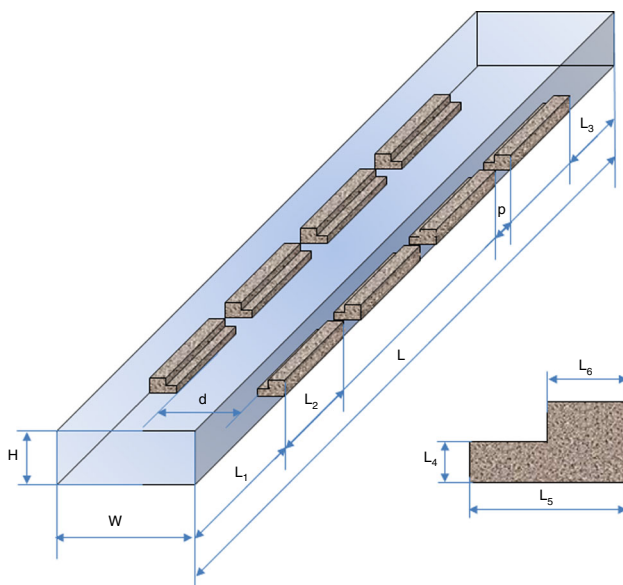


Fig. 1 The studied geometrics in present study

Table 1 The dimensions of problem in this article

Dimension of milichannel	Parameters	Value × 10 – 4/m
Milichannel width	w	5
Milichannel height	H	3
Entrance length	L1	5
Ribbed length	L2	15
Longitudinal distance between two teeth	P	15
Output length	L3	10
Crossing distance between two teeth	d	0.2
Little ribbed height	L4	1
Bigger ribbed width	L5	4.8
Little ribbed width	L6	2

Continuity equation:

$$\frac{\partial}{\partial x}(\rho_{nf}u_c) + \frac{\partial}{\partial y}(\rho_{nf}u_c) = 0 \quad (1)$$

Momentum equations:

$$\begin{aligned} \frac{\partial}{\partial x}(\rho_{nf}u_c u_c) + \frac{\partial}{\partial y}(\rho_{nf}u_c v_c) = & -\frac{\partial p}{\partial x} + \frac{\partial}{\partial x} \left(\mu_{nf} \frac{\partial u_c}{\partial x} \right) \\ & + \frac{\partial}{\partial y} \left(\mu_{nf} \frac{\partial u_c}{\partial y} \right) - \frac{\mu_{nf} u_c}{K} \\ & - \frac{\rho_{nf} F}{\sqrt{K}} |u_c| u_c \end{aligned} \quad (2)$$

$$\begin{aligned} \frac{\partial}{\partial x}(\rho_{nf}u_c v_c) + \frac{\partial}{\partial y}(\rho_{nf}v_c v_c) = & -\frac{\partial p}{\partial y} + \frac{\partial}{\partial x} \left(\mu_{nf} \frac{\partial v_c}{\partial x} \right) \\ & + \frac{\partial}{\partial y} \left(\mu_{nf} \frac{\partial v_c}{\partial y} \right) - \frac{\mu_{nf} v_c}{K} \\ & - \frac{\rho_{nf} F}{\sqrt{K}} |u_c| v_c \end{aligned} \quad (3)$$

Energy equation:

$$\begin{aligned} \frac{\partial}{\partial x}(\rho_{nf}c_{nf}u_c T_c) + \frac{\partial}{\partial y}(\rho_{nf}c_{nf}u_c T_c) \\ = \frac{\partial}{\partial x} \left(k_e \frac{\partial T_c}{\partial x} \right) + \frac{\partial}{\partial y} \left(k_e \frac{\partial T_c}{\partial y} \right) \end{aligned} \quad (4)$$

Nanofluid properties

The main purpose of this study is investigating the effect of nanofluid on heat transfer rate inside the microchannel with L-shaped porous ribs. In this study, water is base fluid and CuO nanoparticles were used with volume fractions of 2 and 4%. In this simulation, nanofluid is homogeneous and for determining its properties, Ref. [36] was used. Also, maximum increase in water temperature is less than 10% that it's not necessary to consider the variation of

Table 2 The properties of Water–CuO nanofluid [36]

$\phi/\%$	$\rho/\text{kg m}^{-3}$	$C_p/\text{J kg}^{-1} \text{K}^{-1}$	$k/\text{W m}^{-1} \text{K}^{-1}$	$\mu/\text{Pa s}$
0	997.1	4.179e3	0.613	891e-6
2	1155.8	3.5925e3	0.7496	1100e-6
4	1314.5	3.1477e3	0.8918	1300e-6

properties and Ref. [36] is the same. The nanofluid properties in different volume fractions are presented in Table 2.

Equations related to the measured parameters

The friction coefficient is a parameter for investigating microchannel performance and depends on the geometrical parameters of microchannel and it can be calculated via following equation [37],

$$f = 2\Delta P \frac{D_h}{L} \frac{1}{\rho u_{in}^2} \tag{5}$$

where D_h is the hydraulic diameter, L is the length of channel, ρ is the density and u_{in} is the inlet velocity. The average Nusselt number is calculated as [38],

$$Nu_{ave} = \frac{q'' D_h}{k_f (T_w - T_m)} \tag{6}$$

In the above equation, T_w is the temperature of microchannel wall and T_m is the average bulk temperature. The performance evaluation criterion (PEC) is defined as follows [39–41],

$$PEC = \frac{\left(\frac{Nu_{ave}}{Nu_{ave,s}}\right)}{\left(\frac{f}{f_s}\right)^{(1/3)}} \tag{7}$$

Geometries, meshing and boundary conditions

In present research, the flow and heat transfer were studied inside the microchannel with the length of 12 mm using finite volume method. According to Fig. 2, for simulating the flow inside the channel, the inlet velocity boundary condition was used for the inlet of channel and for the channel outlet; the pressure boundary condition was applied. Also, on the microchannel walls, the no-slip boundary condition was used. Regarding the symmetric channel, half of microchannel was modeled and the symmetrical boundary condition was applied to the middle plane. According to Fig. 2, the used ribs are away from the

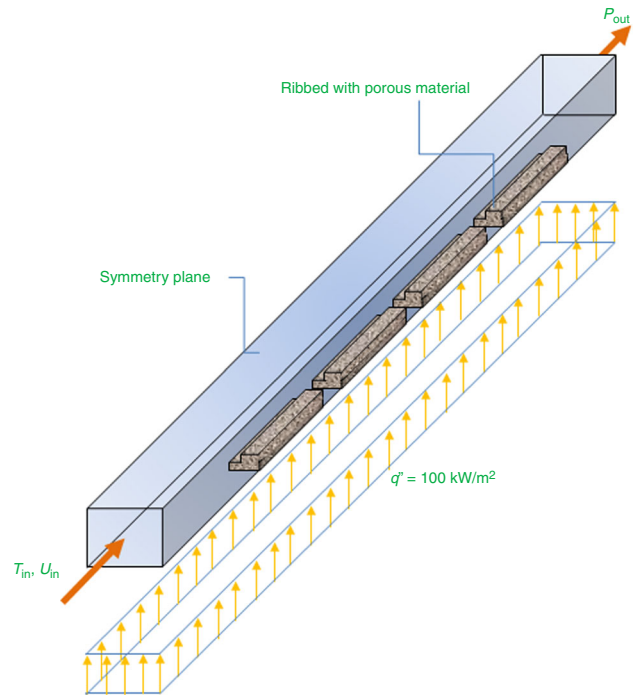


Fig. 2 The boundary conditions in the present numerical simulation

Table 3 Grid independency—the changes of average Nusselt number with the number of elements

Number of grid	average Nusselt number	Error/%
25,000	12.98	47.2
45,000	13.67	40.5
60,000	16.59	15.8
100,000	18.99	1.2
250,000	19	1
300,000	19.015	Best grid

center of channel and by employing the symmetrical boundary condition, there is a space for crossing the working fluid between two ribs. Therefore, the ribs used in this research are L-shaped. Also, the microchannel wall is under the constant heat flux of $100,000 \text{ W m}^{-2}$ and the nanofluid flow was simulated for Reynolds numbers of 100, 300, 600 and 1200 with volume fractions of 0, 2 and 4%. In order to investigate the effect of element number on the numerical results, the results independency from grid is given in Table 3. Based on this table, in the computational cell number of 100,000 (each element is 25 microns), the average Nusselt number is independent from the element number. Therefore, in order to have the minimum effect on the obtained results, this element number was used in all of the simulations.

Numerical procedure

In order to solve the governing equations on flow and heat transfer, the finite volume method was employed. In the numerical solving procedure, for discretizing the governing equations, the second-order discretization and for coupling the velocity and pressure, SIMPLE method was used. Also, the maximum residual of 10^{-6} was considered in the present simulations.

Validation

Yucel and Guven investigated the flow and heat transfer characteristics of laminar flow in a rectangular channel with porous obstacles (with Darcy number of 1×10^{-3}) [42]. They simulated the flow and heat transfer in Reynolds numbers of 100–1500 and thermal conductivity ratios (λ)

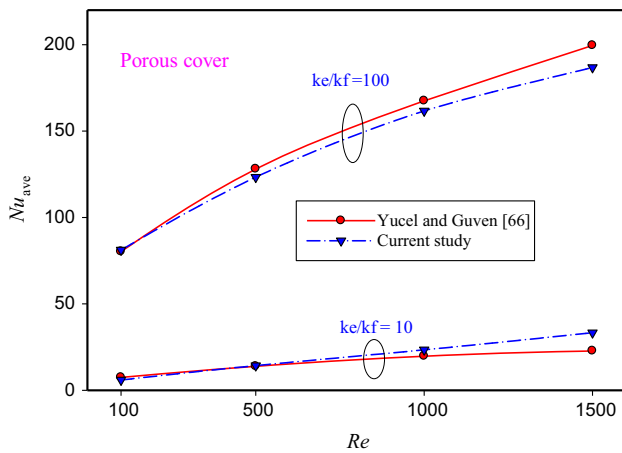


Fig. 3 The validation of numerical results in present study with Ref. [42]

of 1, 10 and 100. In order to validate the accuracy of the current results, the obtained results have been compared with the studies of Yucel and Guven [42] in $\lambda = 10, 100$ with different Reynolds numbers. As seen in Fig. 3, there is an agreeable accordance between the results indicating the accuracy and exactness of current results, that the maximum difference between current results and Yucel and Guven [42] results is 8% at Reynolds number of 1500.

Results and discussions

Microchannel with porous medium ($\varepsilon = 0.8$ and $k = 15 \text{ W m}^{-1} \text{ K}^{-1}$)

The results presented in this section are related to the condition in which the porous medium with thermal conductivity of $k = 15 \text{ W m}^{-1} \text{ K}^{-1}$ and $\varepsilon = 0.8$ was placed inside the microchannel. In the porous medium, the effect of porous material is same as the last terms of momentum equation. In Fig. 4a, the average Nusselt number is presented based on the volume fraction of CuO nanoparticles inside the microchannel. As it can be seen, by increasing Reynolds number, due to the increase in fluid momentum and consequently, the increase in heat transfer, Nusselt number increases. In Fig. 4b, the average Nusselt number as the function of volume fraction of nanoparticles is shown in each of the studied Reynolds numbers. As it is seen, in each of the studied Reynolds number, by increasing volume fraction of nanoparticles, the heat transfer rate (Nusselt number) increases with low inclination, which is because of the increase in heat transfer coefficient by adding nanoparticles. Also, according to the mentioned figure, by increasing Reynolds number and

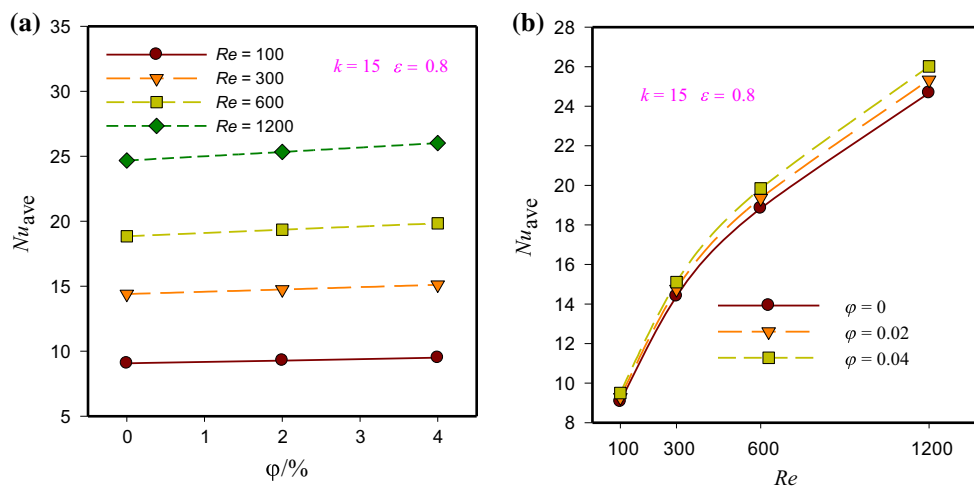


Fig. 4 The average Nusselt number as the function of (a). Volume fraction of nanoparticle and (b). Re number for ($k = 15 \text{ W m}^{-1} \text{ K}^{-1}$, $\varepsilon = 0.8$)

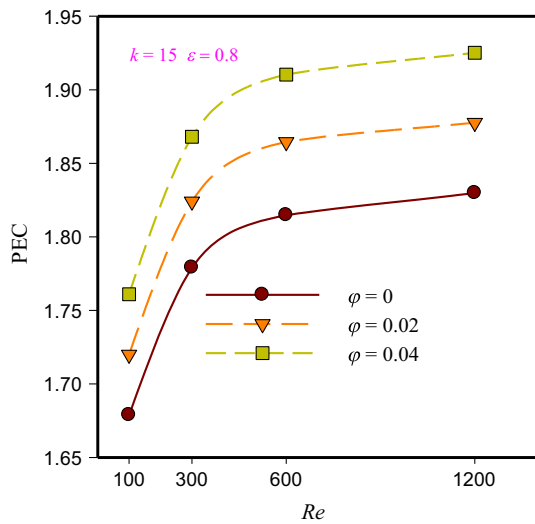


Fig. 5 The changes of PEC as the function of Reynolds number in different volume fractions ($k = 15 \text{ W m}^{-1} \text{ K}^{-1}$, $\epsilon = 0.8$)

volume fraction of nanoparticles, the slope of Nusselt number graph changes. In other words, when the values of Reynolds number and flow momentum are high, by adding more nanoparticles, heat transfer increases. By investigating the average Nusselt number distribution in the studied cases, it is determined that, adding nanoparticles to the working fluid and the existence of porous ribs inside the microchannel cause an increase in heat transfer. It should be noted that the heat transfer increase is an advantage of using nanofluid and porous medium; however, one of the disadvantages of this method is more pressure drop in the system. The PEC of each studied condition was investigated in this section. According to the definition, the performance evaluation criterion is the ratio of heat transfer increase to increasing applied pressure drop to the system. When this coefficient is more than 1, the heat transfer

increase is useful, because the heat transfer increase is more than the pressure drop applied to the system. In Fig. 5, PEC is shown as the function of Reynolds number in the microchannel with porous ribs with $\epsilon = 0.8$ and $k = 15 \text{ W m}^{-1} \text{ K}^{-1}$ for flow with different Reynolds numbers, the pure water fluid and water/CuO nanofluid with volume fractions of 2 and 4%. According to the mentioned figure, by increasing Reynolds number, the value of PEC increases. Therefore, it can be said that using porous medium and nanoparticles in flow with higher Reynolds numbers and in laminar flow regime is more economical. As it can be seen, in a constant Reynolds number, by increasing volume fraction of nanoparticles, PEC increases. Also, the maximum value of PEC was obtained in flow with $Re = 1200$ and 4% volume fraction of nanoparticles.

Microchannel with porous medium ($k = 15 \text{ W m}^{-1} \text{ K}^{-1}$ and $\epsilon = 0.5$)

In this section, the local Nusselt number distribution, the average Nusselt number and PEC of microchannel with porous ribs with $\epsilon = 0.5$ and $k = 15 \text{ W m}^{-1} \text{ K}^{-1}$ were presented for flow with Reynolds numbers of 100, 300, 600 and 1200 and three volume fractions of CuO nanoparticles. In Fig. 6a, the average Nusselt number is shown as the function of Reynolds number for pure water and water/CuO nanofluid with 2 and 4% volume fractions of nanoparticles. According to this figure, by increasing Reynolds number, which causes an increase in fluid momentum, Nusselt number increases. In Fig. 6b, the average Nusselt number as the function of volume fraction is shown in four studied Reynolds numbers. By investigating the local Nusselt number distribution, it is found that

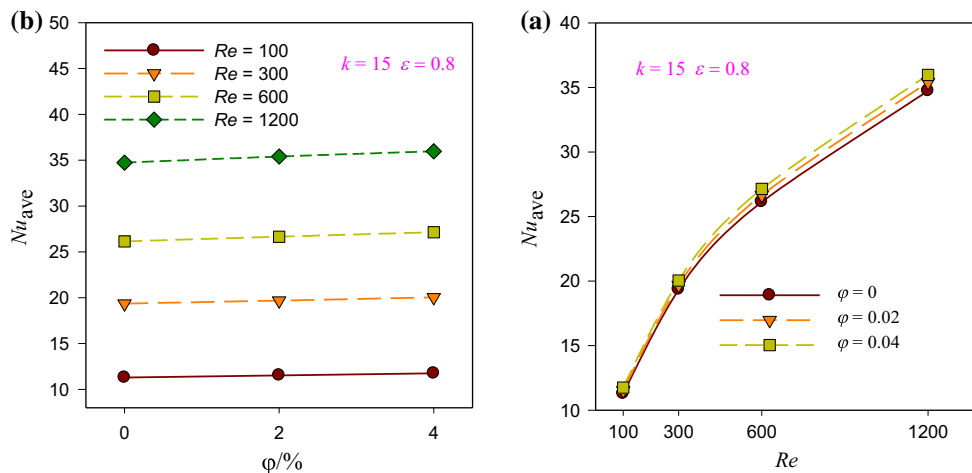


Fig. 6 The average Nusselt number changes as the function of **a** Reynolds number **b** different volume fractions of nanoparticles in ($k = 15 \text{ W m}^{-1} \text{ K}^{-1}$, $\epsilon = 0.8$)

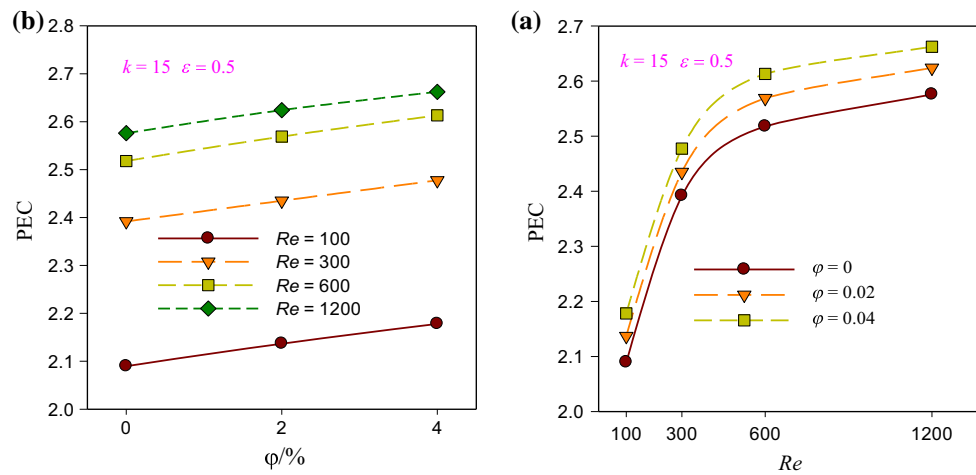


Fig. 7 The changes of PEC as the function of **a** Reynolds number and **b** volume fraction of nanoparticles in different Reynolds numbers in ($k = 15 \text{ W m}^{-1} \text{ K}^{-1}$, $\varepsilon = 0.5$)

Fig. 8 The changes of average Nusselt number as the function of (a) Reynolds number and (b) different volume fraction of nanoparticles for ($k = 7.5 \text{ W m}^{-1} \text{ K}^{-1}$, $\varepsilon = 0.8$)

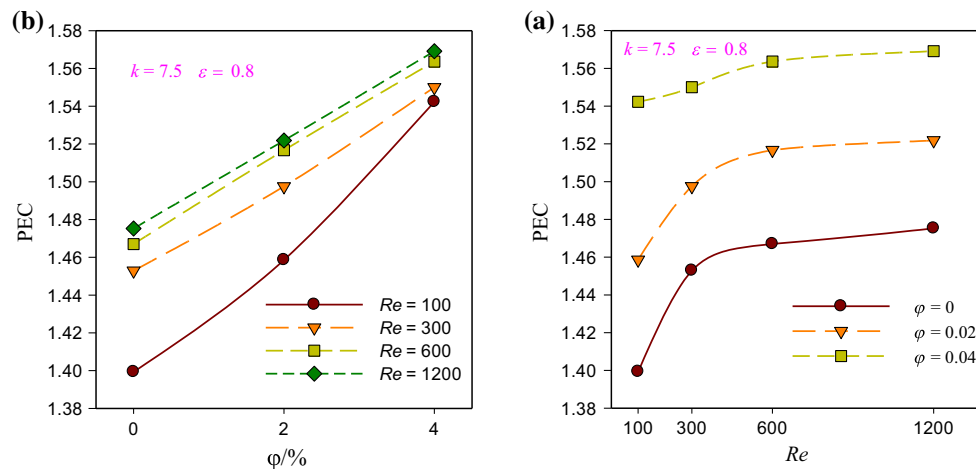
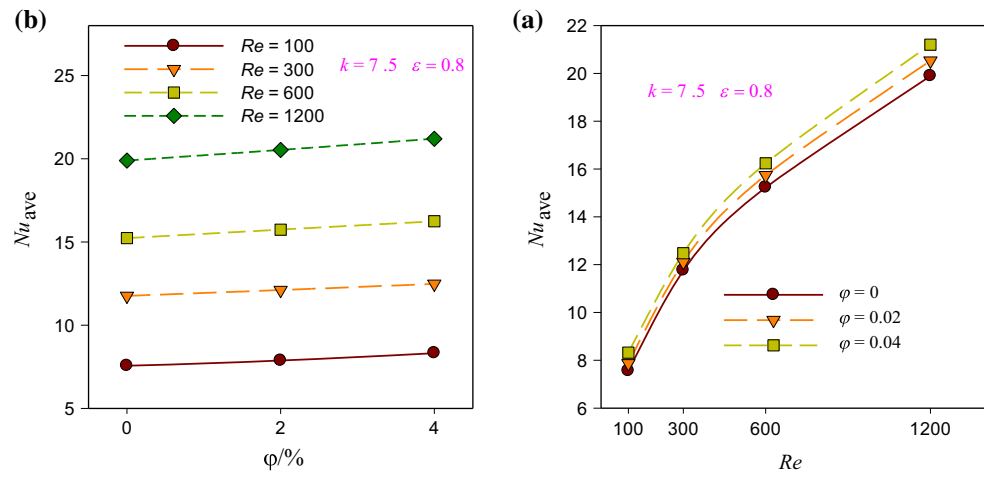


Fig. 9 The changes of PEC as the function of **a** Reynolds number and **b** volume fraction of nanoparticles in different Reynolds numbers ($k = 7.5 \text{ W m}^{-1} \text{ K}^{-1}$, $\varepsilon = 0.8$)

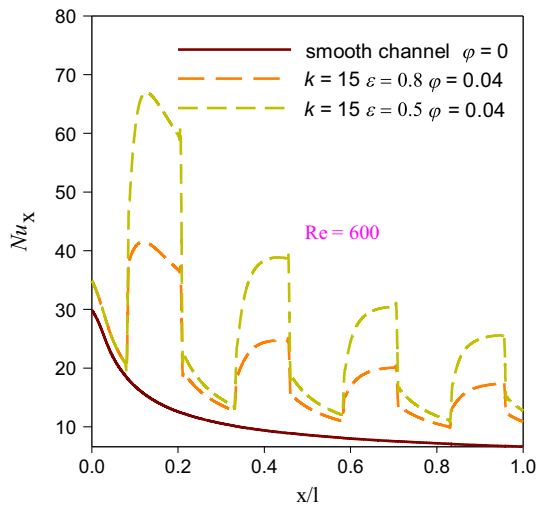


Fig. 10 The local Nusselt number distribution in flow with Reynolds number of 600 in two different porosity coefficients of porous media ($k = 15 \text{ W m}^{-1} \text{ K}^{-1}$)

the increase in volume fraction of nanoparticles has a small effect on Nusselt number increase.

PEC for $k = 15 \text{ W m}^{-1} \text{ K}^{-1}$ and $\epsilon = 0.5$

In Fig. 7a, the performance evaluation criterion as the function of Reynolds number was investigated in microchannel with porous ribs with $\epsilon = 0.5$ and $k = 15 \text{ W m}^{-1} \text{ K}^{-1}$ for the pure water flow and Water/nanofluid with 2 and 4% volume fractions. Based on the mentioned figure, by increasing Reynolds number, PEC increases. This issue indicates that, in flow with higher Reynolds number, the heat transfer increase caused by fluid momentum increase is higher than the pressure drop applied to system. In order to investigate the simultaneous effect of studied volume fraction of nanoparticles and Reynolds numbers, PEC was shown as the function of volume fraction in Fig. 7b. As it is seen, by increasing volume fraction of nanoparticles, PEC increases and the

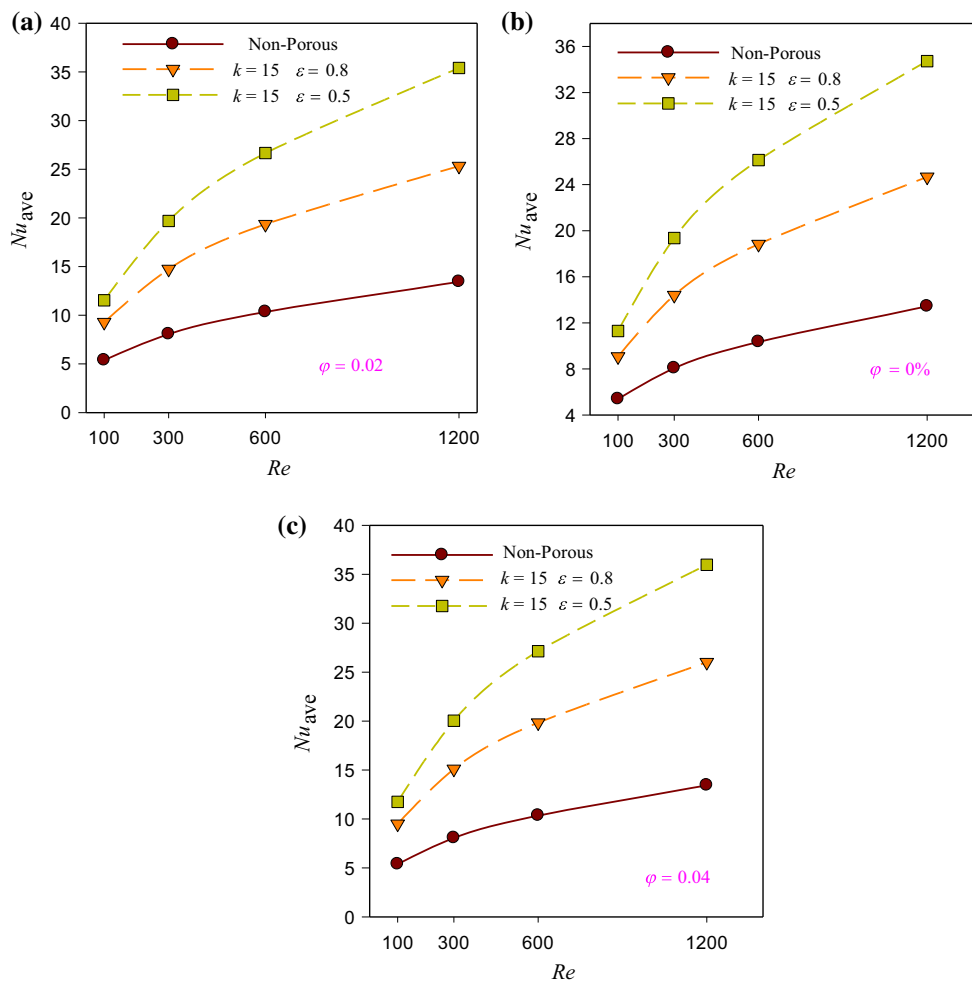


Fig. 11 The average Nusselt number as the function of Reynolds number, porosity coefficient and different volume fractions of solid nanoparticles

heat transfer rate is dominated on the increase in pressure drop applied to the system. Also, in Reynolds number of 1200, by increasing volume fraction of nanoparticles from 0 to 4%, the thermal performance increases up to 3%.

Microchannel with porous medium ($\epsilon = 0.8$ and $k = 7.5 \text{ W m}^{-1} \text{ K}^{-1}$)

The thermal performance of microchannel with porous ribs with $\epsilon = 0.8$ and $k = 7.5 \text{ W m}^{-1} \text{ K}^{-1}$ was investigated in this section. In Fig. 8a, the average Nusselt number as the function of Reynolds number was shown for the pure water fluid and water/CuO nanofluid with 2 and 4% volume fractions. It can be understood from this figure that by increasing Reynolds number of flow, the heat transfer rate and Nusselt number are increased. In Fig. 8b, the average Nusselt number is given as the function of volume fraction of nanoparticles in flow with the studied Reynolds numbers and it is determined that the increasing volume fraction has no effect on the Nusselt number inside the microchannel.

PEC ($k = 7.5 \text{ W m}^{-1} \text{ K}^{-1}$, $\epsilon = 0.8$)

Figure 9a shows PEC for pure water flow and Water/-nanofluid with 2 and 4% volume fractions of nanoparticles as the function of Reynolds number. Based on this figure, by increasing Reynolds number, PEC increases slightly. Figure 9b shows PEC as the function of volume fraction of nanoparticle with different Reynolds numbers. By increasing volume fraction of nanoparticles, especially in flow with Reynolds numbers of 600 and 1200, PEC has higher increase. This behavior shows that, in porous medium, the rate of heat transfer increase is more than increasing pressure drop applied to the system; therefore, the amount of PEC is higher.

The effect of porosity coefficient on thermal performance

In this section, the local Nusselt number distribution, the average Nusselt number and PEC in two porosity

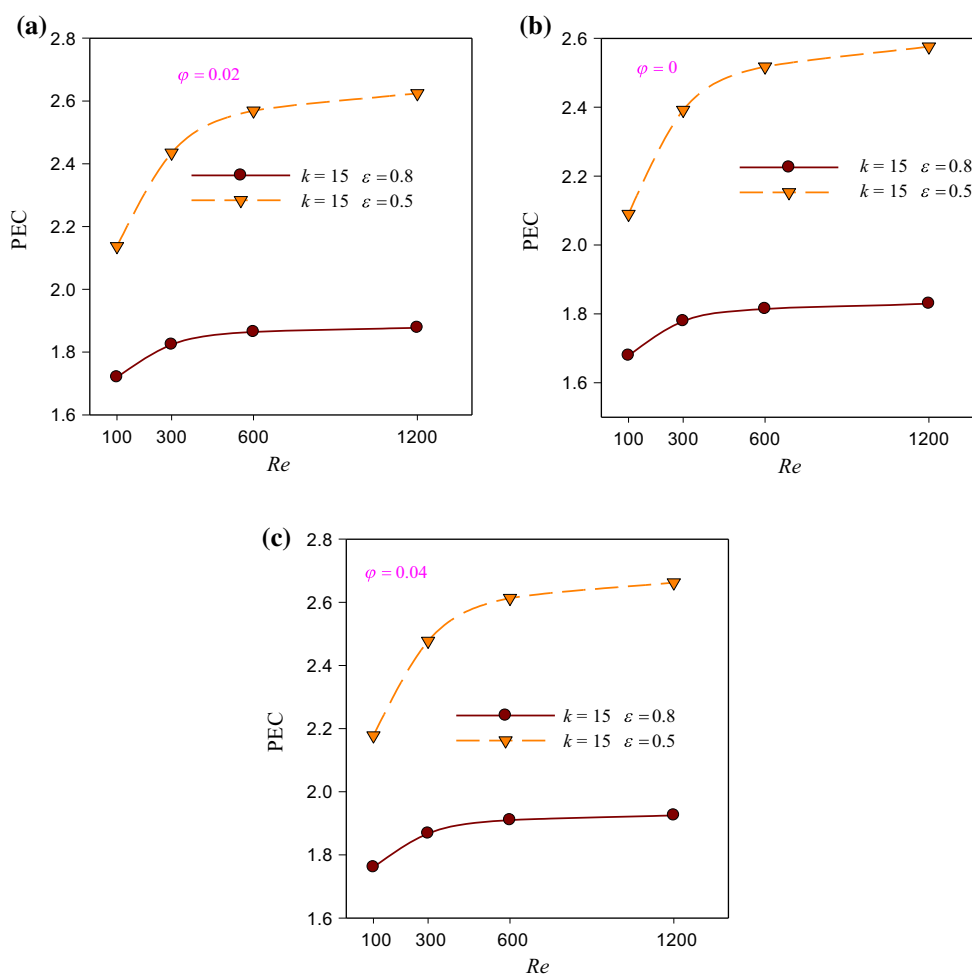


Fig. 12 The PEC as the function of Reynolds number. The effect of porosity coefficient of porous media

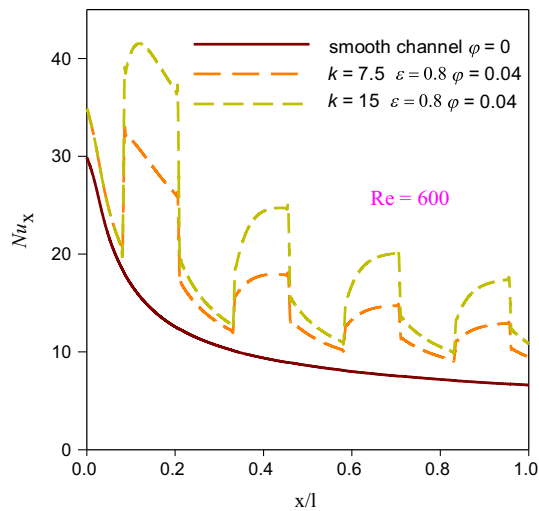


Fig. 13 The distribution of local Nusselt number in flow with Reynolds number of 600 in different thermal conductivity of porous media ($\epsilon = 0.8$)

coefficients of 0.8 and 0.5 in flow with different Reynolds numbers were studied. In order to compare the effect of porosity ratio of porous medium, the distribution of local Nusselt number in flow with Reynolds number of 600 with 4% volume fraction of nanoparticles is shown in Fig. 10. According to this figure, by increasing the porosity coefficient of porous ribs used in microchannel, the local Nusselt number increases significantly, which means that the heat transfer has increased. In order to study the effect of porosity coefficient of porous ribs with the studied Reynolds numbers and volume fractions of nanoparticles, in Fig. 11 the average Nusselt number is shown for the pure water fluid and water/CuO nanofluid with 2 and 4% volume fractions in flat microchannel and the microchannel with porous ribs with two porosity coefficients of 0.5 and 0.8. Based on this figure, the increase in porous medium causes the increase in average Nusselt number; however, in all of the studied Reynolds numbers, the influence of porosity coefficient is not the same. For the pure water flow with Reynolds number of 100, due to the higher of porosity

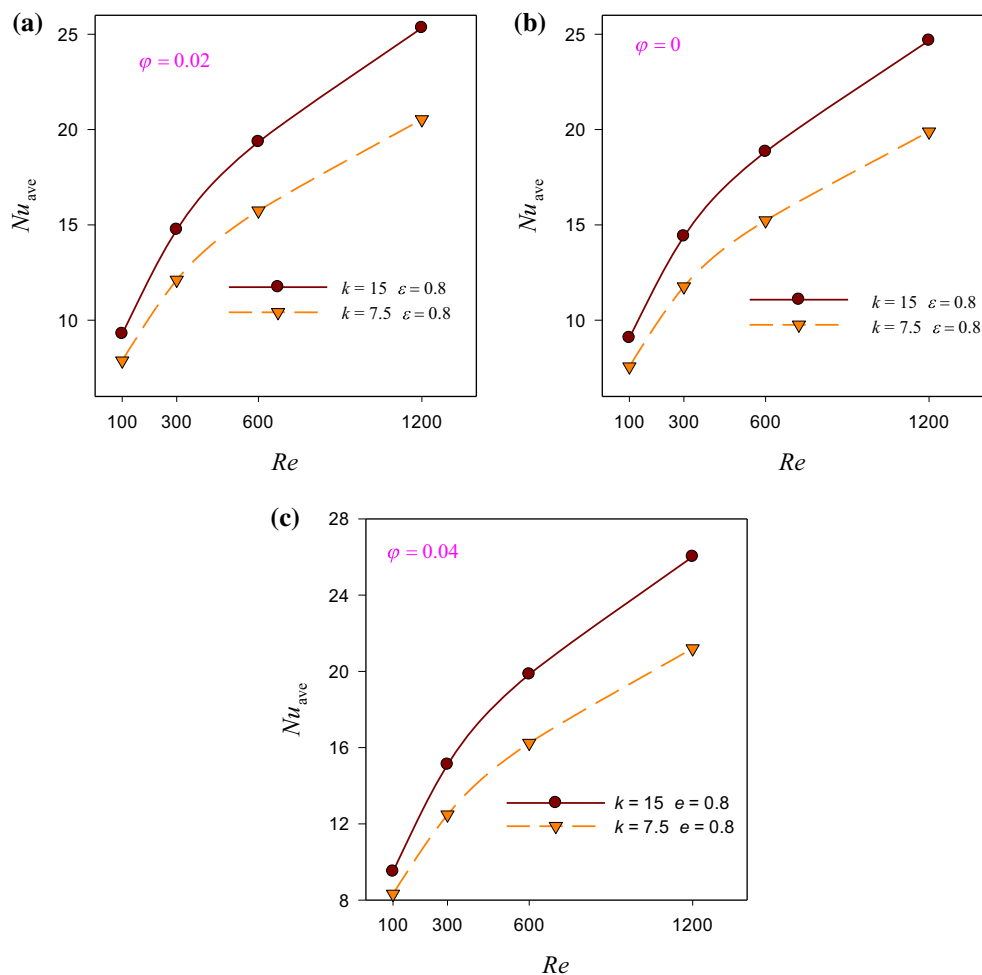


Fig. 14 The average Nusselt number as the function of Reynolds number—the effect of porosity coefficient of porous media and different volume fractions of nanoparticles in ($\epsilon = 0.8$)

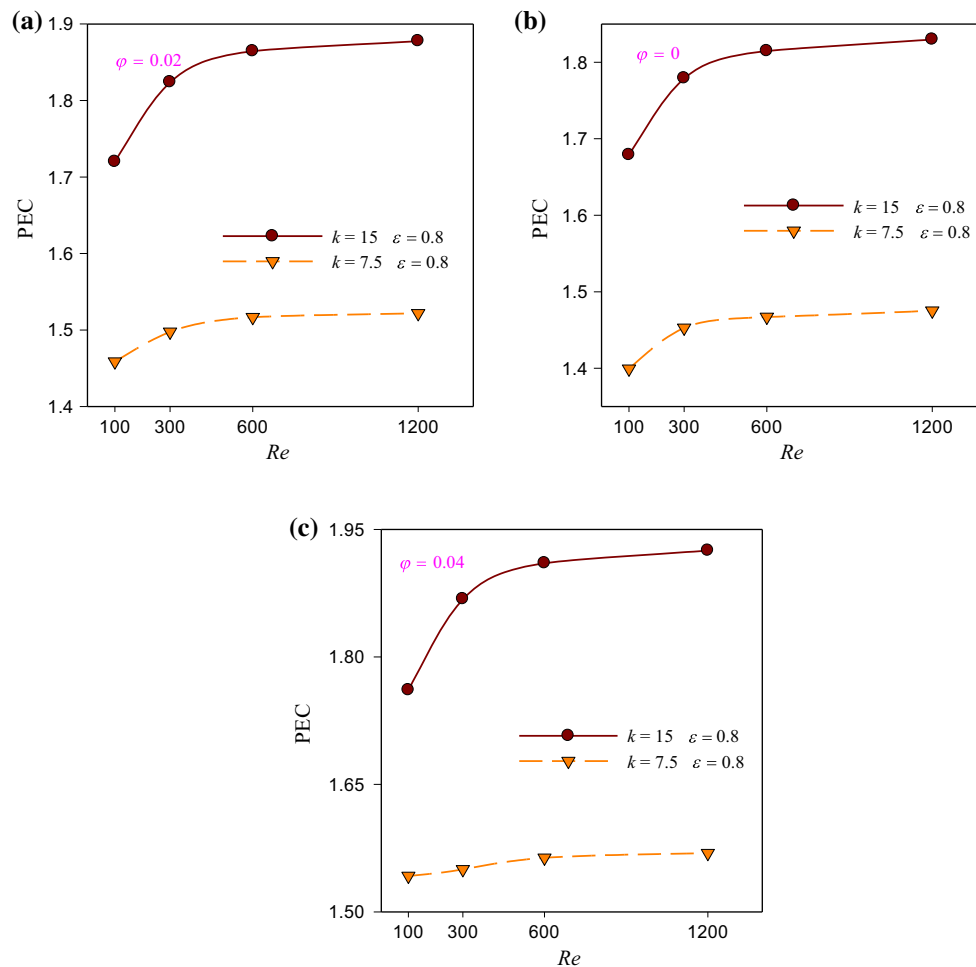


Fig. 15 The PEC as the function of Reynolds number, the effect of porosity coefficient of porous media and volume fraction of nanoparticles ($\varepsilon = 0.8$)

rate, Nusselt number increases from 9 to 11 (approximately 22%), while in flow with Reynolds number of 1200, because of the increase in porosity ratio, the average Nusselt number increases from 13 to 35 (more than 1.5%). It can be concluded that, from the heat transfer perspective (without considering fluid parameters), the use of porous medium with high porosity coefficient is accompanied with more heat transfer increase. According to the presented results, by using porous medium with high porosity ratio the heat transfer increases. However, the increase in porosity ratio of ribs used in microchannel is followed with severe pressure drop. Therefore, investigating the effect of high porosity ratio on PEC is essential. For this reason, in Fig. 12, the PEC of pure water fluid and water/nanofluid with 2 and 4% of CuO nanoparticles was presented. According to this figure, the PEC of microchannel with porosity coefficient of 0.5 is more than the PEC in porosity coefficient of 0.8. Consequently, from the engineering and economics perspectives, using porous medium with high porosity coefficient is logical.

The effect of thermal conductivity of porous medium

In the following, the effect of thermal conductivity of porous ribs on heat transfer rate and PEC was studied. For this reason, the obtained results are presented for two porous media with thermal conductivities of 7.5 and 15 $\text{W m}^{-1} \text{K}^{-1}$ with porosity coefficient of 0.8. Figure 13 illustrates the distribution of local Nusselt number in flow with Reynolds number of 600 for the flat microchannel and the microchannel with porous ribs with two thermal conductivities of 7.5 and 15 $\text{W m}^{-1} \text{K}^{-1}$. As it is observed, by increasing the conduction heat transfer coefficient of porous ribs, the local Nusselt number increases indicating the heat transfer rise. In Fig. 14, the effect of conduction heat transfer coefficient of porous medium on average Nusselt number was studied for the pure water fluid and nanofluid with 2 and 4% volume fractions of CuO nanoparticles, respectively. It is observed that, by increasing the conduction heat transfer coefficient of porous ribs, the average

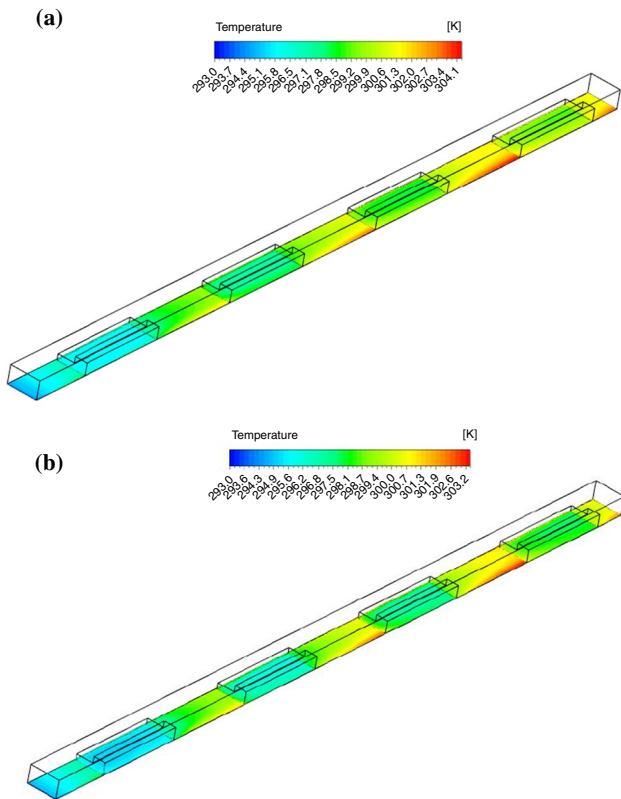


Fig. 16 The contours of temperature distribution of microchannel floor in flow with Reynolds number of 300 and 4% of volume fraction of nanoparticle. **a** $k = 7.5 \text{ W m}^{-1} \text{ K}^{-1}$, $\varepsilon = 0.8$ and **b** $k = 15 \text{ W m}^{-1} \text{ K}^{-1}$, $\varepsilon = 0.8$

Nusselt number increases. Consequently, using porous medium with high thermal conductivity of porous ribs has acceptable thermal performance and heat transfer increase. In order to investigate the effect of conduction heat transfer, coefficients of porous ribs on PEC in pure water flow and nanofluid with 2 and 4% volume fractions are shown in Fig. 15. As it is seen, by increasing the conduction heat transfer coefficient, PEC increases. The notable point is the differences of PEC inclination as the function of Reynolds number in two thermal conductivity coefficients of porous medium. The inclination of PEC changes in porous medium with high thermal conductivity coefficients is more than the low thermal conductivity coefficients. In fact, due to the higher Reynolds number of flow, increasing thermal conductivity coefficient of porous medium and fluid momentum has a significant effect on heat transfer rise.

The effect of porosity ratio and thermal conductivity of porous medium on temperature distribution

In this section, by presenting temperature distribution on microchannel floor in the studied cases, the effects of

Table 4 The effect of porosity coefficient on the Nu/Re

Porosity	Re	Phi	Nu/Re	Increment by porous media/%
No porous	1200	0	0.0112	–
		0.02	0.0114	–
		0.04	0.0115	–
0.8	1200	0	0.0206	83.6
		0.02	0.0211	84.8
		0.04	0.0217	89.0
0.5	1200	0	0.0289	158.4
		0.02	0.0295	163.4
		0.04	0.0300	167.6

Reynolds number, volume fraction of 4%, porosity ratio of porous medium and the conduction heat transfer coefficient were investigated. In Fig. 16, the temperature distribution contours in flow with Reynolds number of 300 and 4% volume fraction of nanoparticles in porous medium with porosity coefficient of 0.8 and thermal conductivity of 15 and $7.5 \text{ W m}^{-1} \text{ K}^{-1}$ are given. By studying the mentioned figure, it can be said that in microchannel with porous medium, due to the high thermal conductivity of porous medium, the temperature of microchannel floor decreases.

The effect of porosity on Re/Nu ratio

In order to investigate the effect of porosity coefficient of porous media, in Table 4, the Nu/Re ratio was presented for the highest value of Reynolds number (1200). As it is seen, by changing the porosity coefficient from 0.8 to 0.5, Nu/Re ratio increases. Investigating the influence of using porous medium and the base fluid on heat transfer shows that the porous medium with porosity coefficients of 0.8 and 0.5 entails the heat transfer increase to 83.6 and 158.4%, respectively. By analyzing the table, it can be understood that the porous medium with porosity coefficient of 0.5 and 4% volume fraction of nanoparticles has the maximum value of heat transfer increase.

Conclusions

In this research, the flow and heat transfer of water/CuO nanofluid in the microchannel with L-shaped porous ribs were numerically investigated. The validation of obtained numerical results with the results of valid references shows the accuracy of present solving procedure. This simulation was carried out in laminar flow regime, and the flow and heat transfer properties were studied in four Reynolds numbers of 100, 300, 600 and 1200 with three volume fractions of CuO nanoparticles. The main purpose of present

study was to investigate the effect of L-shaped porous medium on flow with different Reynolds numbers and volume fractions of water/CuO nanofluid. The obtained results show that the simultaneous use of nanofluid with porous ribs does not have significant influence on heat transfer increase. In Reynolds numbers of 100, 300, 600 and 1200, by increasing the thermal conductivity of porous medium from 7.5 to 15 W m⁻¹ K⁻¹, Nusselt number increases up to 11, 19, 22 and 23%, respectively. Also, in Reynolds numbers of 100, 300, 600 and 1200, by increasing the porosity coefficient from 0.8 to 0.5, the average Nusselt number increases up to 25, 38, 40 and 42%, respectively. Based on the achieved results, the maximum rate of performance evaluation criterion was accomplished in flow with Reynolds number of 1200 in porosity rate of 0.5 and thermal conductivity of 15 W m⁻¹ K⁻¹.

References

- Kuznetsov AV. Analytical studies of forced convection in partly porous configurations. In: Vafai K, editor. Handbook of porous media. Marcel Dekker, Inc; 2005.
- Poulikakos D, Kazmierczak M. Forced convection in a duct partially filled with a porous material. *ASME J Heat Trans.* 1987;109:653–62.
- Alkam MK, Al-Nimr MA, Hamdan MO. Enhancing heat transfer in parallel plate channels by using porous inserts. *Int J Heat Mass Trans.* 2001;44:931–8.
- Alkam MK, Al-Nimr MA. Improving the performance of double-pipe heat exchangers by using porous substrates. *Int J Heat Mass Trans.* 1999;42:3609–18.
- Jiang PX, Ren ZP. Numerical investigation of forced convection heat transfer in porous media using a thermal non-equilibrium model. *Int J Heat Fluid Flow.* 2001;22:102–10.
- Lee DY, Jin JS, Kang BH. Momentum boundary layer and its influence on the convective heat transfer in porous media. *Int J Heat Mass Trans.* 2002;45:229–33.
- Mohamad AA. Heat transfer enhancements in heat exchangers fitted with porous media. Part I: constant wall temperature. *Int J Therm Sci.* 2003;42:385–95.
- Kuznetsov AV. Numerical modeling of turbulent flow in a composite porous/fluid duct utilizing a two-layer k–ε model to account for interface roughness. *Int J Therm Sci.* 2004;43:1047–56.
- Vafai K, Haji-Sheikh A. Analysis of flow and heat transfer in porous media imbedded inside various-shaped ducts. *Int J Heat Mass Trans.* 2004;47:1889–905.
- Forooghi P, Abkar M, Saffar-Avval M. Steady and unsteady heat transfer in a channel partially filled with porous media under thermal non-equilibrium condition. *Transp Porous Med.* 2011;86:177–98.
- Hetsroni G, Gurevich M, Rozenblit R. Sintered porous medium heat sink for cooling of high-power mini-devices. *Int J Heat Fluid Flow.* 2006;27:259–66.
- Yang YT, Hwang ML. Numerical simulation of turbulent fluid flow and heat transfer characteristics in heat exchangers fitted with porous media. *Int J Heat Mass Trans.* 2009;52:2956–65.
- Nazari S, Toghraie D. Numerical simulation of heat transfer and fluid flow of Water–CuO nanofluid in a sinusoidal channel with a porous medium. *Physica E.* 2017;87:134–40.
- Li J, Kleinstreuer C. Thermal performance of nanofluid flow in microchannels. *Int J Heat Fluid Flow.* 2008;29(4):1221–32.
- Chein R, Chuang J. Experimental microchannel heat sink performance studies using nanofluids. *Int J Therm Sci.* 2007;46(1):57–66.
- Barzegarian R, Moraveji MK, Aloueyan A. Experimental investigation on heat transfer characteristics and pressure drop of BPHE (brazed plate heat exchanger) using TiO₂–water nanofluid. *Exp Therm Fluid Sci.* 2016;74:11–8.
- Jung JY, Oh HS, Kwak HY. Forced convective heat transfer of nanofluids in microchannels. *Int J Heat Mass Trans.* 2009;52(1–2):466–72.
- Ho CJ, Wei LC, Li ZW. An experimental investigation of forced convective cooling performance of a microchannel heat sink with Al₂O₃–Water nanofluid. *Appl Therm Eng.* 2010;30(2–3):96–103.
- Bhattacharya P, Samanta AN, Chakraborty S. Numerical study of conjugate heat transfer in rectangular microchannel heat sink with Al₂O₃–H₂O nanofluid. *Heat Mass Trans.* 2009;45(10):1323–33.
- Sheikhzadeh GA, Ebrahim Qomi M, Hajialigol N, Fattahi A. Effect of Al₂O₃–Water nanofluid on heat transfer and pressure drop in a three-dimensional microchannel. *Int J Nano Dimens.* 2013;3(4):281–8.
- Abdollahi A, Mohammed HA, Vanaki ShM, Osia A, Golbahar Haghighi MR. Fluid flow and heat transfer of nanofluids in microchannel heat sink with V-type inlet/outlet arrangement. *Alex Eng J.* 2016. <https://doi.org/10.1016/j.aej.2016.09.019>.
- Lelea D. The performance evaluation of Al₂O₃/Water nanofluid flow and heat transfer in microchannel heat sink. *Int J Heat Mass Trans.* 2011;54:3891–9.
- Sakanova A, Keian CC, Zhao J. Performance improvements of microchannel heat sink using wavy channel and nanofluids. *Int J Heat Mass Trans.* 2015;89:59–74.
- Rimbault B, Nguyen CT, Galanis N. Experimental investigation of CuO–Water nanofluid flow and heat transfer inside a microchannel heat sink. *Int J Therm Sci.* 2014;84:275–92.
- Li P, Zhang D, Xie Y. Heat transfer and flow analysis of Al₂O₃–Water nanofluids in microchannel with dimple and protrusion. *Int J Heat Mass Trans.* 2014;73:456–67.
- Diao YH, Liu Y, Wang R, Zhao YH, Guo L, Tang X. Effects of nanofluids and nanocoatings on the thermal performance of an evaporator with rectangular microchannels. *Int J Heat Mass Trans.* 2013;67:183–93.
- Mital M. Analytical analysis of heat transfer and pumping power of laminar nanofluid developing flow in microchannels. *Appl Therm Eng.* 2013;50(1):429–36.
- Ming TZ, Zheng Y, Liu J, Liu C, Liu W, Huang SY. Heat transfer enhancement by filling metal porous medium in central area of tubes. *J Energy Inst.* 2010;83(1):17–24.
- Peng C, Ming T, Tao Y. Thermal and hydraulic performances of a tube filled with various thermal conductivities of porous media. *Int J Heat Mass Trans.* 2015;81:784–96.
- Akbari OA, Toghraie D, Karimipour A. Impact of ribs on flow parameters and laminar heat transfer of Water–Aluminum oxide nanofluid with different nanoparticle volume fractions in a three-dimensional rectangular microchannel. *Adv Mech Eng.* 2016;7:1–11.
- Shamsi MR, Akbari OA, Marzban A, Toghraie D, Mashayekhi R. Increasing heat transfer of non-Newtonian nanofluid in rectangular microchannel with triangular ribs. *Physica E.* 2017;93:167–78.
- Akbari OA, Toghraie D, Karimipour A, Marzban A, Ahmadi GR. The effect of velocity and dimension of solid nanoparticles on

- heat transfer in non-Newtonian nanofluid. *Physica E*. 2017; 86:68–75.
33. Alipour H, Karimipour A, Safaei MR, Semiromi DT, Akbari OA. Influence of T-semi attached rib on turbulent flow and heat transfer parameters of a silver–Water nanofluid with different volume fractions in a three-dimensional trapezoidal microchannel. *Physica E*. 2016;88:60–76.
 34. Akbari OA, Karimipour A, Toghraie D, Safaei MR, Alipour Goodarzi MH, Dahari H. Investigation of rib's height effect on heat transfer and flow parameters of laminar water–Al₂O₃ nanofluid in a two dimensional rib-microchannel. *Appl Math Comp*. 2016;290:135–53.
 35. Nojoomizadeh M, Karimipour A. The effects of porosity and permeability on fluid flow and heat transfer of multi walled carbon nano tubes suspended in oil (MWCNT/Oil nano fluid) in a microchannel filled with a porous medium. *Phys E Low Dimens Syst Nanostruct*. 2016. <https://doi.org/10.1016/j.physe.2016.07.020>.
 36. Akbari OA, Toghraie D, Karimipour A. Numerical simulation of heat transfer and turbulent flow of Water nanofluids copper oxide in rectangular microchannel with semi attached rib. *Adv Mech Eng*. 2016;8(4):1–25.
 37. Hosseinnezhad R, Akbari OA, Hassanzadeh Afrouzi H, Biglarian M, Koveiti A, Toghraie D. The numerical study of heat transfer of turbulent nanofluid flow in a tubular heat exchanger with twin twisted-tapes inserts. *J Therm Anal Calorim*. 2018. <https://doi.org/10.1007/s10973-017-6900-5>.
 38. Parsaiemehr M, Pourfattah F, Akbari OA, Toghraie D, Sheikhzadeh Gh. Turbulent flow and heat transfer of Water/Al₂O₃ nanofluid inside a rectangular ribbed channel. *Physica E*. 2018;96:73–84.
 39. Heydari M, Toghraie D, Akbari OA. The effect of semi-attached and offset mid-truncated ribs and Water/TiO₂ nanofluid on flow and heat transfer properties in a triangular microchannel. *Therm Sci Eng Prog*. 2017;2:140–50.
 40. Gholami MR, Akbari OA, Marzban A, Toghraie D, Ahmadi Sheikh Shabani GHR, Zarringhalam M. The effect of rib shape on the behavior of laminar flow of oil/MWCNT nanofluid in a rectangular microchannel. *J Therm Anal Calorim*. 2017. <https://doi.org/10.1007/s10973-017-6902-3>.
 41. Gravndyan Q, Akbari OA, Toghraie D, Marzban A, Mashayekhi R, Karimi R, Pourfattah F. The effect of aspect ratios of rib on the heat transfer and laminar water/TiO₂ nanofluid flow in a two-dimensional rectangular microchannel. *J Mol Liq*. 2017;236: 254–65.
 42. Yuçel N, Guven RT. Numerical study of heat transfer in a rectangular channel with porous covering obstacles. *Transp Porous Med*. 2009;77:41–58. <https://doi.org/10.1007/s11242-008-9260-6>.